Theory of dark resonances for alkali-metal vapors in a buffer-gas cell

A. V. Taĭchenachev,[1,2,3] V. I. Yudin,[1,2,3] R. Wynands,[4,*] M. Stähler,[4] J. Kitching,[3] and L. Hollberg[3]
[1]*Novosibirsk State University, Pirogova 2, Novosibirsk 630090, Russia*
[2]*Institute of Laser Physics SD RAS, Novosibirsk 630090, Russia*
[3]*Time and Frequency Division, NIST Boulder, 325 South Broadway, Boulder, Colorado 80305*
[4]*Institut für Angewandte Physik, Universität Bonn, Wegelerstraße 8, D-53115 Bonn, Germany*
(Received 7 October 2002; published 21 March 2003)

We develop an analytical theory of dark resonances that accounts for the full atomic-level structure, as well as all field-induced effects such as coherence preparation, optical pumping, ac Stark shifts, and power broadening. The analysis uses a model based on relaxation constants, which assumes the total collisional depolarization of the excited state. A good qualitative agreement with the experiments for Cs in Ne is obtained.

DOI: 10.1103/PhysRevA.67.033810 PACS number(s): 42.50.Gy, 32.70.Jz, 32.80.Bx, 33.70.Jg

I. INTRODUCTION

Nonlinear interference effects connected with the atomic ground-state coherence are now well known and widely used [1]. One of the most promising classes of these effects, especially for precise measurements, is that of supernarrow dark resonances [2–4] that appear in the medium's response to bichromatic laser excitation when the laser frequency difference is close to the atomic ground-state splitting. The use of vapor cells containing a buffer gas in addition to an alkali-metal vapor has allowed the measurement of resonance linewidths less than 50 Hz [5,6]. While such resonances have been extensively investigated experimentally (especially in the case of Cs) [2], a detailed theoretical understanding is not yet well developed for realistic multilevel systems, motivating the present work. Our theory was developed in close connection with ongoing efforts to construct compact atomic clocks [3,7–9] and magnetometers [2,4]. For any practical application of dark resonances, the stability and accuracy are optimized with respect to parameters such as the output signal amplitude, the width, and the shift. In the problem considered here, many parameters, such as laser detunings, field component polarizations and amplitudes, and buffer-gas pressure, affect the dark resonance itself. In addition, various excitation schemes (for example, D_2 versus D_1 line excitation [10]) and different atomic isotopes can be used. A natural question arises: what design will optimize the performance of the clock (or magnetometer)? Previous theories did not completely answer this question. One main obstacle was connected with the complicated energy-level structure of the real atomic systems used in the experiments.

Generally speaking, there are several types of problems in the theoretical description of dark resonances. One problem relates to a proper treatment of the relaxation processes in the system, including velocity-changing collisions [11] and the spatial diffusion of coherently prepared atoms [12,13]. Light propagation through coherently prepared nonlinear media, especially through optically thick media [14], can be thought of as another type of difficulty. This paper addresses another important problem of field-induced processes in multilevel systems such as coherence preparation, optical pumping, ac Stark shifts, and power broadening. All existing theories can be classified into three kinds: few-state models (basically, three-state Λ systems) [6,15,16], perturbation theories [17], and numerical simulations [6,15]. All three classes of theories have disadvantages. The first theory neglects many details of the actual configuration of atomic levels. Perturbation theory neglects some effects induced by the presence of the optical field (namely, optical pumping, ac Stark shifts, and power broadening). Numerical simulation theories demonstrate a lack of genuine understanding and predictive power.

This paper presents an analytical theory that accounts for the level structure (both Zeeman and hyperfine) of a real atom, as well as all field-induced effects. The relaxation processes are treated in the simplest way: by neglecting velocity-changing collisions and all effects connected with the spatial inhomogeneity, we reduce the model to the one described simply by relaxation constants. The crucial assumption is total collisional depolarization of the excited state. In addition, we add the (optional) approximations of homogeneous broadening and low saturation. With these approximations, a general analytical result is obtained for the atomic response, which result is valid for arbitrary excitation schemes (D_2 as well as D_1 lines), light field polarizations, and magnetic fields. In the specific case of circularly polarized light in the presence of a magnetic field, where only two states participate in the coherence preparation, analytical line shapes (generalized Lorentzian) coincide exactly with the phenomenological model heuristically introduced previously to fit experimental data [18]. In the case of zero magnetic field, and when the contributions of different Zeeman substates are well overlapped, the resonance line shape is also approximately described by the generalized Lorentzian. A comparison of analytically calculated coefficients of the model (with no free parameters) with coefficients extracted from the experimental data demonstrates a good qualitative agreement.

II. STATEMENT OF THE PROBLEM

In this section, the general framework of the problem is described, the basic assumptions we make are stated, and the

*Present address: Département de Physique, Université de Fribourg, Chemin du Musée 3, 1700 Fribourg, Switzerland.

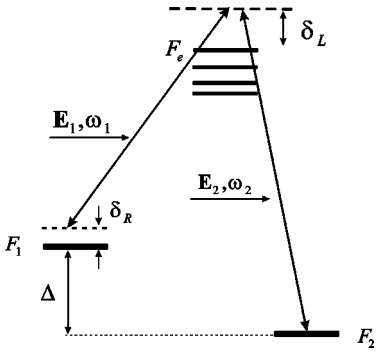

FIG. 1. Excitation scheme.

specific procedure for calculating the quantities of interest is outlined. We consider the resonant interaction of alkali-metal atoms in the $S_{1/2}$ ground state with a two-frequency laser field

$$\mathbf{E}(z,t)=\mathbf{E}_1\exp[-i(\omega_1 t-k_1 z)]+\mathbf{E}_2\exp[-i(\omega_2 t-k_2 z)]+\text{c.c.}, \quad (1)$$

where both components propagate in the positive direction ($k_{1,2}>0$). The field can excite atoms either to the $P_{1/2}$ state (D_1 line) or to the $P_{3/2}$ state (D_2 line). Two hyperfine (HF) components are present in the ground state with the total angular momenta $F_1=I+1/2$ and $F_2=I-1/2$ (where I is the nuclear spin). The HF splitting in the ground state, $\Delta=(\mathcal{E}_1-\mathcal{E}_2)/\hbar$, is in the range 1–10 GHz. The excited state has two (D_1 line) or four (D_2 line) HF levels with the angular momenta $F_e=I-J_e,\ldots,I+J_e$ and the energies $\mathcal{E}_e=\hbar\omega_e$. The HF splitting of the excited state is typically one order of magnitude smaller than Δ. To be more specific, we assume that the frequency ω_1 is close to resonance with the $F_1\rightarrow F_e$ transitions, while the other frequency ω_2 is close to the frequencies of the $F_2\rightarrow F_e$ transitions. Thus, we have a Λ-type excitation scheme (Fig. 1). In the absence of an external B field, the HF levels are degenerate with respect to the total angular-momentum projections. For the Zeeman substates, the following shorthand notations will be used: $|e\rangle=|F_e,m_e\rangle$ with $m_e=-F_e,\ldots,F_e$, and $|i,m\rangle=|F_i,m\rangle$ with $m=-F_i,\ldots,F_i (i=1,2)$.

For simplicity, we consider first an atom at rest, positioned at the origin ($z=0$). Each frequency component of the field can, in principal, induce transitions from both ground-state HF levels. Then the interaction Hamiltonian in the dipole approximation contains contributions of two kinds:

$$\hat{H}_{D-E}=-\sum_{e,i,m}|e\rangle\langle e|(\hat{\mathbf{d}}\cdot\mathbf{E}_i)|i,m\rangle\langle i,m| -\sum_{e,i\neq j,m}|e\rangle\langle e|(\hat{\mathbf{d}}\cdot\mathbf{E}_i)|j,m\rangle\times\langle j,m|e^{-i(\omega_i-\omega_j)t}+\text{H.c.}, \quad (2)$$

where we use a rotating frame (the unitary transformation of the ground-state basis $|i,m\rangle\rightarrow\exp(i\omega_i t)|i,m\rangle$), and $\hat{\mathbf{d}}$ is the dipole moment operator. The first term in Eq. (2) is independent of time in the rotating basis, and we refer to it as the resonant contribution. The second term, oscillating at the difference frequency, results in the off-resonant contributions to the optical shifts and optical pumping rates, as well as in temporal oscillations of the atomic density matrix. The role of the off-resonant term in the case of a three-level Λ system has been studied in great detail [16]. The amplitudes of the oscillating parts of the density matrix can be approximated as $|dE|^2/(\hbar\Delta)^2$. For the moderate field intensities considered here (<10 mW/cm^2), this ratio is very small, $|dE|^2/(\hbar\Delta)^2\sim10^{-6}-10^{-8}$, and the oscillating terms can be safely neglected. However, the off-resonant contributions to the optical energy shifts and widths can be significant, especially in the case of large one-photon detunings.

Hamiltonian for a free atom in the rotating frame can be written as

$$\hat{H}_0=-\sum_e\hbar(\delta_L-\omega_e)|e\rangle\langle e|-\hbar\frac{\delta_R}{2}\times\sum_m(|1,m\rangle\langle 1,m|-|2,m\rangle\langle 2,m|). \quad (3)$$

Here $\delta_L=(\delta_1+\delta_2)/2$ is the average one-photon detuning, δ_L and ω_e are measured from a common zero level (for example, from the HF level with maximal momentum $F_e=I+J_e$), and $\delta_R=\delta_2-\delta_1=\omega_2-\omega_1-\Delta$ is the Raman (two-photon) detuning.

Since this paper is concerned with the field-induced effects in multilevel atomic systems, the relaxation processes are modeled by several constants. The homogeneous broadening of the optical line, due mainly to collisions with a buffer gas, is described by the constant γ. We assume that the excited state is completely depolarized due to collisions during the radiative lifetime τ_e, i.e., the depolarization rates γ_κ obey the condition

$$\gamma_\kappa\,\tau_e\gg 1. \quad (4)$$

The relaxation of the ground-state density matrix to the isotropic equilibrium, both due to the diffusion through the laser beam and due to collisions, is modeled by a single constant Γ.

Under the assumption of moderate field intensities and high buffer-gas pressure, we develop the theory in the low-saturation limit:

$$\frac{|dE|^2}{\hbar^2}\ll\frac{\gamma}{\tau_e}. \quad (5)$$

The two-photon dark resonance appears when the Raman detuning δ_R is scanned around zero. The width of the dark resonance, which is related to the ground-state relaxation, is usually six orders of magnitude smaller than the optical linewidth γ. The approximation $\delta_R\ll\gamma$ is therefore suitable.

It should be stressed that all approximations are well justified for typical experimental conditions. For example, in the case of Cs in a background Ne atmosphere at a pressure

of $p=10$ kPa, the homogeneous broadening $\gamma \approx 2\pi 860$ MHz [19] of the optical line exceeds the Doppler width $k\bar{v} \approx 2\pi 300$ MHz, so velocity-changing collisions are inconsequential. The collisional depolarization rate $\gamma_\kappa \approx 2\pi 70$ MHz [20] is large compared to the inverse radiative lifetime $1/\tau_e = 2\pi 5.3$ MHz. The Rabi frequency $|dE|/\hbar \approx 1/\tau_e$ for the field intensity 8.8 mW/cm^2, which results in a saturation parameter $(|dE|/\hbar)^2 \tau_e/\gamma \approx 10^{-2}$. The two-photon detuning is scanned in the range $|\delta_R| < 2\pi 1$ MHz, and the ground-state relaxation rate can be estimated to be $\Gamma \approx 2\pi 53$ Hz [12,21].

Eliminating optical coherences with these approximations (for details see the Appendix), we arrive at the following set of equations for the ground-state density submatrix ($\hat{\sigma}_{gg} = \hat{\Pi}_g \hat{\sigma} \hat{\Pi}_g$):

$$\frac{d}{dt}\hat{\sigma}_{gg} = -i[\hat{H}_{\rm eff}\hat{\sigma}_{gg} - \hat{\sigma}_{gg}\hat{H}_{\rm eff}{}^\dagger] + \left(\frac{\pi_e}{\tau_e} + \Gamma\right)\frac{\hat{\Pi}_g}{n_g}, \quad (6)$$

$$\mathrm{Tr}\{\hat{\sigma}_{gg}\} = 1, \quad (7)$$

where $\hat{\Pi}_g = \Sigma_m(|1,m\rangle\langle 1,m| + |2,m\rangle\langle 2,m|)$ is the ground-state projector, $n_g = 2(2I+1)$ is the total number of substates in the ground state, and π_e is the total population of the excited state. The first term ($\propto \pi_e$) of the source in Eq. (6) corresponds to the isotropic repopulation of the ground-state sublevels due to the spontaneous decay of the excited states. The other term ($\propto \Gamma$) describes the entrance of unpolarized atoms due to diffusion and collisions. Due to the conservation of the total number of particles (7), separate dynamic equations for the excited-state density-matrix elements are not needed. Both the dynamics and steady state are completely governed by the non-Hermitian ground-state Hamiltonian:

$$\hat{H}_{\rm eff} = -\frac{\delta_R}{2}\sum_m (|1,m\rangle\langle 1,m| - |2,m\rangle\langle 2,m|) + \hat{R} - i\frac{\Gamma}{2}\hat{\Pi}_g. \quad (8)$$

Here the excitation matrix

$$\hat{R} = \sum_{i,j,e,m,m'} |i,m\rangle \frac{\langle i,m|(\hat{\mathbf{d}}\cdot\mathbf{E}_i)^\dagger|e\rangle\langle e|(\hat{\mathbf{d}}\cdot\mathbf{E}_j)|j,m'\rangle}{\hbar^2[(\delta_L - \omega_e) + i\gamma/2]}\langle j,m'| + \sum_{i\neq j,e,m,m'} |i,m\rangle \frac{\langle i,m|(\hat{\mathbf{d}}\cdot\mathbf{E}_j)^\dagger|e\rangle\langle e|(\hat{\mathbf{d}}\cdot\mathbf{E}_j)|i,m'\rangle}{\hbar^2[(\delta_L + \omega_j - \omega_i - \omega_e) + i\gamma/2]} \times \langle i,m'| \quad (9)$$

contains the resonant (first summation) as the well as the off-resonant (second summation) contributions to the optical shifts and optical pumping rates (Hermitian and anti-Hermitian parts, respectively). The nondiagonal ($i \neq j$) elements of the resonant term induce the Raman coherence between the HF levels of the ground state responsible for the dark resonance.

The generic matrix element in Eq. (9) is calculated from the Wigner-Eckart theorem:

$$\begin{aligned}\langle i,m_i|(\hat{\mathbf{d}}\cdot\mathbf{E}_k)^\dagger|e\rangle\langle e|(\hat{\mathbf{d}}\cdot\mathbf{E}_l)|j,m_j\rangle &= |\langle J_e||d||J_g\rangle|^2\, r(F_e,F_i)\, r(F_e,F_j) \\ &\times \sum_{K,q} (-1)^{F_e+F_j+K} \\ &\times \begin{Bmatrix} 1 & 1 & K \\ F_i & F_j & F_e \end{Bmatrix} \sqrt{2K+1}(-1)^{F_i-m_i} \\ &\times \begin{pmatrix} F_i & K & F_j \\ -m_i & q & m_j \end{pmatrix} \{\mathbf{E}_k^* \otimes \mathbf{E}_l\}_{K\,q}, \end{aligned} \quad (10)$$

where $\langle J_e||d||J_g\rangle$ is the reduced matrix element of the dipole moment and

$$r(F_e,F_i) = \sqrt{(2J_e+1)(2F_e+1)(2F_i+1)} \begin{Bmatrix} J_g & J_e & 1 \\ F_e & F_i & I \end{Bmatrix}$$

is the partial coupling amplitude of the $F_i \to F_e$ transition. In the general case, we have scalar ($K=0$), vector ($K=1$), and quadrupole ($K=2$) contributions. All possible selection rules are contained in the coefficients of vector coupling, i.e., the $6j$ and $3jm$ symbols.

For an atom moving along the direction of propagation of the optical field, the field frequencies are shifted due to the Doppler effect, $\omega_i \to \omega_i - k_i v$. As a result, a Doppler shift of the one-photon detuning $\delta_L \to \delta_L - kv$ occurs, where $k = (k_1 + k_2)/2$, as does a residual Doppler shift of the Raman detuning $\delta_R \to \delta_R - (k_2 - k_1)v$. At high buffer-gas pressure the residual Doppler shift is suppressed due to the Lamb-Dicke effect [12,22]. However, in the general case the Doppler shift of the one-photon detuning can be significant, and certain quantities must be averaged over the Maxwell velocity distribution. Nevertheless, for buffer-gas pressures typically used in experiments, the approximation of homogeneous broadening is reasonable, as a first approach to the problem, because the homogeneous width γ equals or even exceeds the Doppler width $k\bar{v}$.

Here we consider the steady-state regime, setting $(d/dt)\hat{\sigma}_{gg} = 0$ in Eq. (6). As a spectroscopic signal, we consider the total excited-state population π_e which is proportional to the total light absorption in optically thin media or to the total fluorescence. The following procedure is used to find π_e. From Eq. (6), the ground-state density matrix $\hat{\sigma}_{gg}$ is expressed in terms of π_e, and then π_e is calculated from the normalization condition (7). The solution of this algebraic problem can be obtained in a compact analytical form in two important special cases. The first arises when both field components have the same simple (circular or linear) polarization and there is no magnetic field. Here, for a suitable choice of the quantization axis, the excitation matrix $\hat{R}$ contains only diagonal elements with respect to the magnetic quantum number, i.e., $m = m'$ in Eq. (9). The second case appears when a magnetic field is applied and just a few substates contribute to the Raman coherence for arbitrary light polarizations and arbitrary magnetic-field directions. Both cases are considered below.

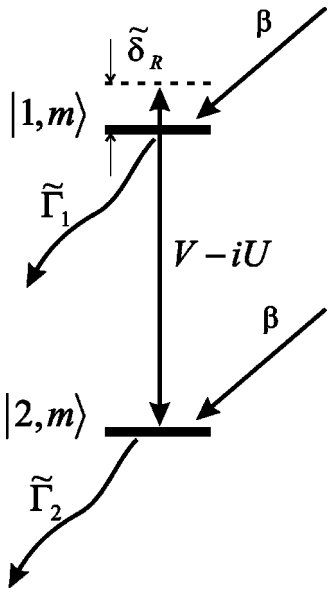

FIG. 2. Effective two-level system, corresponding to one m block.

III. SIMPLE LIGHT POLARIZATION (NO MAGNETIC FIELD)

We turn now to the case of circular field polarization, when the quantization axis is directed orthogonal to the polarization vector (or alternatively linear polarization when the quantization axis is aligned along the polarization vector). We evaluate the total excited-state population π_e in order to determine how the dark resonance signal (proportional to π_e) depends on parameters such as the optical detuning from resonance. Under these assumptions, the complete set of equations (6) can be split into independent blocks for each magnetic quantum number m (m blocks). These blocks for $m=\pm F_1$ contain only one equation for the substate population $\pi^{(\pm F_1)}$. The other blocks with $m\neq\pm F_1$ contain four equations (two for the populations and two for the Raman coherences), corresponding to an effective two-level system with the upper $|1,m\rangle$ and lower $|2,m\rangle$ states (Fig. 2). The parameters of the two-level system are expressed in terms of matrix elements of $\hat{R}$ as follows: the population relaxation rates $\tilde{\Gamma}_i=\Gamma+R_i^{(m)}$ include the optical pumping rates $R_i^{(m)}=2\,\mathrm{Im}\{\langle i,m|\hat{R}|i,m\rangle\}$; the dephasing rate is $\tilde{\Gamma}_{12}=(\tilde{\Gamma}_1+\tilde{\Gamma}_2)/2$; the effective detuning $\tilde{\delta}_R=\delta_R-(S_1^{(m)}-S_2^{(m)})$ includes optical shifts $S_i^{(m)}=\mathrm{Re}\{\langle i,m|\hat{R}|i,m\rangle\}$; and the coherence between levels is excited by the complex coupling $V-iU=\langle 1,m|\hat{R}|2,m\rangle$. Note that the phase of the matrix element $\langle 1,m|(\hat{\mathbf{d}}\cdot\mathbf{E}_1)^{\dagger}|e\rangle\langle e|(\hat{\mathbf{d}}\cdot\mathbf{E}_2)|2,m\rangle$ can be chosen equal to zero without loss of generality, so that $\langle 2,m|\hat{R}|1,m\rangle=\langle 1,m|\hat{R}|2,m\rangle$.

Both the upper and lower states are repopulated with the same rate $\beta=(\pi_e/\tau_e+\Gamma)/n_g$. First the total m-block population $\pi^{(m)}=\pi_1^{(m)}+\pi_2^{(m)}$ per unit repopulation rate is found. For the outermost blocks, $m=\pm F_1$, $\pi^{(\pm F_1)}=1/(\Gamma+R_1^{(\pm F_1)})$. The result for $m\neq\pm F_1$ is a quotient of polynomials of second order in the effective detuning,

$$\pi^{(m)}=\frac{A\,\tilde{\delta}_R^2+B}{C\,\tilde{\delta}_R^2+D\tilde{\delta}_R+E}, \tag{11}$$

where

$$A=\tilde{\Gamma}_1+\tilde{\Gamma}_2,\quad B=\tilde{\Gamma}_{12}[\tilde{\Gamma}_{12}(\tilde{\Gamma}_1+\tilde{\Gamma}_2)+8\,V^2];$$
$$C=\tilde{\Gamma}_1\tilde{\Gamma}_2,\quad D=4\,UV(\tilde{\Gamma}_1-\tilde{\Gamma}_2); \tag{12}$$
$$E=\tilde{\Gamma}_{12}^2\tilde{\Gamma}_1\tilde{\Gamma}_2+2\,\tilde{\Gamma}_{12}(\tilde{\Gamma}_1+\tilde{\Gamma}_2)(V^2-U^2)-16\,U^2V^2.$$

The repopulation rate, corresponding to unit total population in all m blocks, is

$$\beta=\left[\sum_{m=-F_1}^{F_1}\pi^{(m)}\right]^{-1}, \tag{13}$$

and the total excited-state population is finally expressed as

$$\pi_e=\tau_e(n_g\beta-\Gamma). \tag{14}$$

In the general case, when polarizations of the field components are different, or the same but elliptical, there is no basis where the matrices $\langle 1,m|\hat{R}|1,m'\rangle$, $\langle 2,m|\hat{R}|2,m'\rangle$, and $\langle 1,m|\hat{R}|2,m'\rangle$ are simultaneously diagonal. In this situation, the full equation set for the ground-state density-matrix elements must be solved, including all possible Zeeman and Raman coherences. Nevertheless, one important exception should be noted. If the optical linewidth is much greater than the excited-state HF splitting $\gamma\gg(\omega_{e,\,\max}-\omega_{e,\,\min})$, the quadrupole contributions to $\hat{R}$ are negligible [17]. The vector terms are diagonal (with respect to the magnetic quantum number) in the coordinate frame with z as the quantization axis, since $[\mathbf{E}_i^*\times\mathbf{E}_j]\propto\mathbf{e}_z$. Thus, we return to the case discussed above.

IV. DARK RESONANCES IN A MAGNETIC FIELD

In a weak magnetic field, the ground-state magnetic sublevels are split due to the linear Zeeman effect, which can be described by the following additional term in the effective Hamiltonian (8):

$$\hat{H}_B=\sum_{i,m}m\Omega_i|i,m\rangle\langle i,m|. \tag{15}$$

Here the quantization axis is directed along the magnetic field, and $\Omega_i=\mu_B g_i B/\hbar$ are the Zeeman splitting frequencies with μ_B the Bohr magneton and B the magnetic flux density. The g factors of levels g_i are expressed through the electronic g_J and nuclear g_I Lande factors:

$$g_{1,2}=\pm\frac{g_J-g_I}{2\,I+1}+g_I.$$

The magnetic field causes a precession of atomic coherences with frequencies $m\,\Omega_i-m'\,\Omega_j$. When the Zeeman frequen-

cies are much larger than the off-diagonal elements of the excitation matrix $\Omega_i \gg |\langle i,m|\hat{R}|i,m'\rangle|$, the light-induced Zeeman coherences within the ith HF level are negligible. Thus, we again have a set of independent two-level systems, consisting of the substates $|1,m_1\rangle$ and $|2,m_2\rangle$ (where $|m_1 - m_2| \leqslant 2$ due to the selection rules). The formulas (11) and (12) for the total block population are still valid for every (m_1, m_2) block with the following substitutions:

$$\tilde{\Gamma}_i = \Gamma + R_i^{(m_i)},$$

$$\tilde{\delta}_R = \delta_R - (S_1^{(m_1)} - S_2^{(m_2)}) - (m_1\Omega_1 - m_2\Omega_2);$$

$$V - iU = \langle 1,m_1|\hat{R}|2,m_2\rangle = \langle 2,m_2|\hat{R}|1,m_1\rangle. \qquad (16)$$

If the Zeeman frequencies significantly exceed the widths $\tilde{\Gamma}_i$, the Zeeman-split dark resonances are well resolved. In other words, the Raman coherence between the substates $|1,m_1\rangle$ and $|2,m_2\rangle$ is effectively induced when the precession frequency is approximately equal to the Raman detuning $\delta_R \approx m_1\,\Omega_1 - m_2\,\Omega_2$. This condition can be simultaneously satisfied for only a few (m_1, m_2) blocks. More precisely, the nuclear Lande factor is typically three orders of magnitude smaller than the electronic Lande factor (for cesium $g_J/g_I \approx 2500$); then, with good accuracy, $\Omega_1 = -\Omega_2 = \Omega$ and the Zeeman shift of the dark resonance position is proportional to the sum of magnetic quantum numbers $n\Omega = (m_1 + m_2)\,\Omega$. It can be seen that, in the general case, three blocks (m, m), $(m-1, m+1)$, and $(m+1, m-1)$ contribute to the coherence preparation for the resonances with even shifts $2\,m\,\Omega$, and two other blocks $(m-1, m)$ and $(m, m-1)$ contribute for the resonances with odd shifts $(2\,m-1)\,\Omega$. When δ_R is tuned around the resonance with given shift $n\,\Omega$, the repopulation rate β can be written as

$$\beta = \left[Z + \sum_{m_1+m_2=n} \pi^{(m_1,m_2)}(\tilde{\delta}_R) \right]^{-1},$$

where the first summand Z does not depend on the Raman detuning:

$$Z = \sum_{m_1+m_2\neq n} \left(\frac{1}{\Gamma + R_1^{(m_1)}} + \frac{1}{\Gamma + R_2^{(m_2)}} \right),$$

and $\pi^{(m_1,m_2)}$ is the total population of the (m_1, m_2) block. Owing to the nuclear contribution, a further increase of the magnetic field causes the dark resonances to be eventually split into individual peaks, corresponding to each (m_1, m_2) block [23].

V. THE RESONANCE LINE SHAPE

We now consider the dark resonance line shape in more detail. First, we analyze the particular case in which just two substates $|1,0\rangle$ and $|2,0\rangle$ participate in the Raman coherence, i.e., we consider the magnetically insensitive resonance $(m=0)$ in a magnetic field. This $(0,0)$ resonance is of primary interest for possible clock applications [2,3,7] because it is only sensitive to a magnetic field in second order. Here the absorption signal n''_{DR} has the form

$$n''_{DR} = \frac{\pi_e}{\tau_e\, n_g} = \frac{1}{Z + \pi^{(0)}(\tilde{\delta}_R)} - \frac{\Gamma}{n_g},$$

$$Z = \sum_{m\neq 0} \left(\frac{1}{\Gamma + R_1^{(m)}} + \frac{1}{\Gamma + R_2^{(m)}} \right), \qquad (17)$$

where $\pi^{(0)}$ is the total population of the $(m=0)$ block per unit repopulation rate [see Eqs. (11) and (12)]. Since $\pi^{(0)}$ is a quotient of polynomials of second order in δ_R, the absorption can be written as the sum of an absorptive Lorentzian and a dispersive Lorentzian, and a constant background:

$$n''_{DR} = -C_1 \frac{(\tilde{\gamma}/2)^2}{(\tilde{\gamma}/2)^2 + (\delta_R - \delta_0)^2} + C_2 \frac{(\delta_R - \delta_0)\,\tilde{\gamma}/2}{(\tilde{\gamma}/2)^2 + (\delta_R - \delta_0)^2} + \text{const.} \qquad (18)$$

The parameters in Eq. (18) are expressed in terms of the coefficients introduced by Eq. (12) in the following way. The dark resonance position is governed by the optical shifts and an additional term caused by the two-photon coupling between levels:

$$\delta_0 = (S_1^{(0)} - S_2^{(0)}) + x, \quad x = -\frac{DZ}{2\,(A + CZ)}. \qquad (19)$$

The width of dark resonance reads

$$(\tilde{\gamma}/2)^2 = \frac{B + EZ}{A + CZ} - x^2. \qquad (20)$$

The amplitudes of the symmetrical and antisymmetrical Lorentzians are found from the relations

$$C_1(\tilde{\gamma}/2)^2 = \frac{BC - AE - xAD}{(A + CZ)^2}, \qquad (21)$$

$$C_2\tilde{\gamma}/2 = \frac{AD}{(A + CZ)^2}. \qquad (22)$$

The background constant $C/(CZ + A) - \Gamma/n_g$ corresponds to the absorption far off the two-photon resonance.

The result (18) for the resonance line shape is quite general. In fact, it does not depend on our simplified assumptions on the relaxation processes, but is valid also in the low-saturation limit for arbitrary relaxation matrix, whenever only two states participate in the coherence preparation and $\delta_R \ll \gamma$.

Turning to the case of zero magnetic field and simple field polarization, we proceed with the goal of determining the resonance position, width, and amplitudes of the symmetrical and asymmetrical components as above. Since all Zeeman levels within a given hyperfine level are now degenerate, we rewrite the repopulation rate β (13) as

$$\beta=[Z+(2F_2+1)\langle\tilde{\pi}^{(m)}(\delta_R)\rangle_m]^{-1}, \tag{23}$$

where

$$Z=\sum_{m=-F_1}^{m=F_1}\left(\frac{1}{\Gamma+R_1^{(m)}}+\frac{1}{\Gamma+R_2^{(m)}}\right)$$

does not depend on δ_R and corresponds to the absorption far off the two-photon resonance; the sum of the variable parts of the m block populations $\tilde{\pi}^{(m)}(\delta_R)$ is expressed through the average over m-blocks, where the average of a variable X is defined as

$$\langle X^{(m)}\rangle_m=\frac{1}{2F_2+1}\sum_{m=-F_2}^{m=F_2}X^{(m)}.$$

Since $\tilde{\pi}^{(m)}(\delta_R)$ is a quotient of polynomials of second order,

$$\tilde{\pi}^{(m)}(\delta_R)=\frac{a_2^{(m)}\delta_R+b_2^{(m)}}{\delta_R^2+a_1^{(m)}\delta_R+b_1^{(m)}},$$

$$a_1^{(m)}=\frac{D}{C}-(S_1^{(m)}-S_2^{(m)}),$$

$$b_1^{(m)}=\frac{E}{C}-(S_1^{(m)}-S_2^{(m)})\frac{D}{C}+(S_1^{(m)}-S_2^{(m)})^2,$$

$$a_2^{(m)}=\frac{A\,D}{C^2},\quad b_2^{(m)}=\frac{B\,C-A\,E+A\,D\,(S_1^{(m)}-S_2^{(m)})}{C^2}, \tag{24}$$

the average $\langle\tilde{\pi}^{(m)}(\delta_R)\rangle_m$ is a quotient of polynomials of order $2\,(2F_2+1)$. Generally this average describes a superposition of resonances with different widths and positions due to the m-dependent power broadening and ac Stark shifts, but if the laser detuning is not too large, $|\delta_L|\leqslant\Delta$, all resonances are well overlapped, and the average $\langle\tilde{\pi}^{(m)}(\delta_R)\rangle_m$ can be approximated by a quotient of polynomials of second order. Here we use the following simple procedure, where the average of a quotient is substituted by a quotient of the averages:

$$\langle\tilde{\pi}^{(m)}(\delta_R)\rangle_m\approx\alpha\frac{\langle a_2^{(m)}\rangle_m\delta_R+\langle b_2^{(m)}\rangle_m}{\delta_R^2+\langle a_1^{(m)}\rangle_m\delta_R+\langle b_1^{(m)}\rangle_m}, \tag{25}$$

and where the correction factor α is chosen such that the exact and approximate expressions coincide at $\delta_R=0$, i.e.,

$$\alpha=\frac{\langle b_1^{(m)}\rangle_m}{\langle b_2^{(m)}\rangle_m}\left\langle\frac{b_2^{(m)}}{b_1^{(m)}}\right\rangle_m.$$

Our approximation for β yields an error less than a few percent across a wide range of parameters. With this approximation, we return to the resonance line shape (18), where the parameters are expressed in terms of the averages over m:

$$\delta_0=-\frac{\langle a_1^{(m)}\rangle_m}{2}-\frac{(2F_2+1)\,\alpha}{Z}\frac{\langle a_2^{(m)}\rangle_m}{2},$$

$$(\tilde{\gamma}/2)^2=\langle b_1^{(m)}\rangle_m+\frac{(2F_2+1)\,\alpha}{Z}\langle b_2^{(m)}\rangle_m-\delta_0^2,$$

$$C_1\,(\tilde{\gamma}/2)^2=(2F_2+1)\,\alpha\frac{\langle b_2^{(m)}\rangle_m+\langle a_2^{(m)}\rangle_m\delta_0}{Z^2},$$

$$C_2\,(\tilde{\gamma}/2)=(2F_2+1)\,\alpha\frac{\langle a_2^{(m)}\rangle_m}{Z^2},$$

$$\text{const}=\frac{1}{Z}-\frac{\Gamma}{n_g}. \tag{26}$$

VI. COMPARISON WITH EXPERIMENT

The analytical line shape (18) coincides exactly with the phenomenological model heuristically introduced previously to fit experimental data [18]. In those experiments a vertical-cavity surface-emitting laser was modulated at the 9.2-GHz hyperfine splitting frequency of the cesium atom, so that the laser output spectrum contained modulation sidebands at this frequency. Using the carrier and one of the sidebands, the dark resonance could be prepared and spectroscopically observed as a function of detuning δ_L of the laser frequency from optical resonance. Data were taken for three different power ratios of the carrier and sideband, with the cesium atoms contained in a cell with 8.7 kPa of neon as a buffer gas. Detection used a modulation technique that allowed to extract simultaneously the absorption and the dispersion line shape [24]. For each detuning δ_L, both line shapes were simultaneously fitted by the model function (18), with C_1, C_2, $\tilde{\gamma}$, and δ_0 as free parameters. Actually, as far as the line shapes themselves are concerned, this is a two-parameter fit: C_2/C_1 and $\tilde{\gamma}$ describe the shape, and the rest the overall amplitude and position of the dark line.

Since these experimental data for Cs in Ne are fitted by Eq. (18) quite well, we can compare analytically calculated coefficients of the generalized Lorentzian to those extracted from the experimental data. The dependence of the coefficients on the total light intensity $\mathcal{I}\propto|E_1|^2+|E_2|^2$ is almost trivial, at least when the power broadening $(R_1^{(m)}+R_2^{(m)})/2$ exceeds the dephasing rate Γ in zero field—all the parameters C_1, C_2, δ_0, and $\tilde{\gamma}$ scale as $\mathcal{I}$. Thus, the most representative test is provided by the dependence of the coefficients on the one-photon detuning δ_L and on the intensity ratio $\mathcal{R}=|E_1|^2/|E_2|^2$ between the two field components. Such comparisons with experimental fit parameters from Ref. [18] are presented in Figs. 3–6, where C_1, C_2, δ_0, and $\tilde{\gamma}$ are plotted as functions of δ_L for three different relative intensities, $\mathcal{R}$. The other parameters used in the calculations correspond to the experimental conditions: excitation by σ^+ polarized radiation, total intensity $\mathcal{I}=0.4$ mW/cm^2, optical linewidth $\gamma=2\pi 750$ MHz, and ground-state relaxation rate $\Gamma=2\pi 150$ Hz. We use no free parameters, just a single

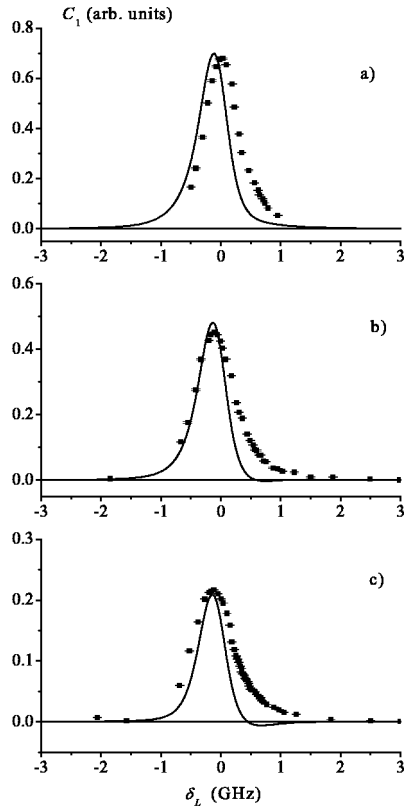

FIG. 3. Absorptive coefficient C_1 versus optical detuning δ_L. Plots (a), (b), and (c) are for $\mathcal{R}=2.4$, 7.2, and 22, respectively. The solid lines indicate the theoretical predictions, while the points indicate the experimental data taken from Ref. [18].

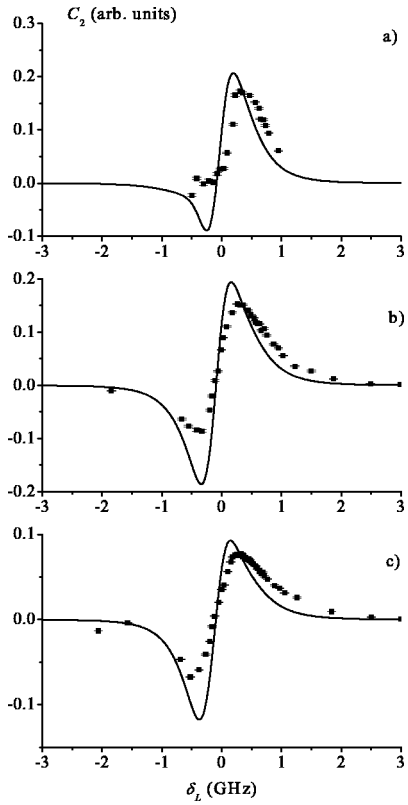

FIG. 4. Dispersive coefficient C_2 versus optical detuning, δ_L. Plots (a), (b), and (c) are for $\mathcal{R}=2.4$, 7.2, and 22, respectively. The solid lines indicate the theoretical predictions, while the points indicate the experimental data.

trivial scaling factor for C_1 and C_2 and a constant offset for δ_0 that accounts for the collisional shift of the dark resonance position.

We see a good qualitative agreement, especially for the resonance position δ_0 and for the width $\tilde{\gamma}$. There are some noticeable discrepancies for the amplitudes C_1 and C_2. In particular, we can see that the theoretical curve for C_1 can cross the zero level at large δ_L, which can be attributed to the well-known Raman absorption, but is not observed in the experimental data.

VII. D_2 LINE EXCITATION AND CONNECTION TO PREVIOUSLY EXISTING THEORIES

In the specific case of the D_2 line of Cs at high buffer-gas pressure, the two-photon amplitudes U and V are much smaller than the optical pumping rates $R_i^{(0)}$ and the optical shifts $S_i^{(0)}$, respectively, because the most probable optical transitions $F_1 \to F_e = I + J_e$ and $F_2 \to F_e = I - J_e$ contribute to the one-photon transitions but not to the two-photon Raman coupling. Note that the ratio between V and $R_i^{(0)}$ can be arbitrary, depending on the one-photon detuning δ_L. As a result, the part of the absorption signal that varies with δ_R is small compared to the constant one, and we arrive, to lowest orders, at the following approximate expressions. The parameter

$$x \approx -\frac{D}{2C} = \frac{2(\tilde{\Gamma}_1 - \tilde{\Gamma}_2)UV}{\tilde{\Gamma}_1 \tilde{\Gamma}_2}$$

is negligible with respect to the other contributions in δ_0, $\tilde{\gamma}$, and C_1. The resonance position offset and the width are approximated as

$$\delta_0 \approx S_1^{(0)} - S_2^{(0)},$$

$$(\tilde{\gamma}/2)^2 \approx \frac{E}{C} \approx \tilde{\Gamma}_{12}^2 + \frac{(\tilde{\Gamma}_1 + \tilde{\Gamma}_2)^2}{\tilde{\Gamma}_1 \tilde{\Gamma}_2} V^2. \tag{27}$$

The amplitudes C_1 and C_2 are given by Eqs. (21) and (22) with $x=0$ and $\tilde{\gamma}$ from Eq. (27).

These results can be compared with those for a three-level Λ system in the low-saturation limit. Our formulas (18)–(22) will describe this last case, as well, if we set $Z=0$, i.e.,

$$\delta_0 = S_1^{(0)} - S_2^{(0)}, \quad (\tilde{\gamma}/2)^2 = \frac{B}{A} = \tilde{\Gamma}_{12}^2 + 4V^2,$$

$$C_1(\tilde{\gamma}/2)^2 = \frac{BC - AE}{A^2}, \quad C_2 \tilde{\gamma}/2 = \frac{D}{A}. \tag{28}$$

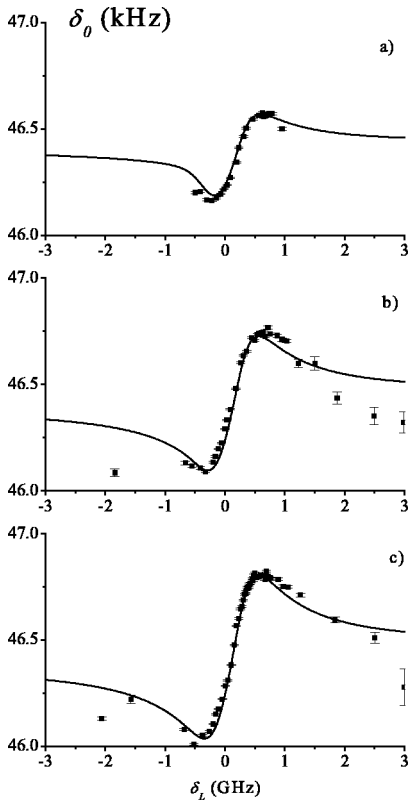

FIG. 5. Frequency shift δ_0 versus optical detuning δ_L. Plots (a), (b), and (c) are for $\mathcal{R}=2.4$, 7.2, and 22, respectively. The solid lines indicate the theoretical predictions, while the points indicate the experimental data.

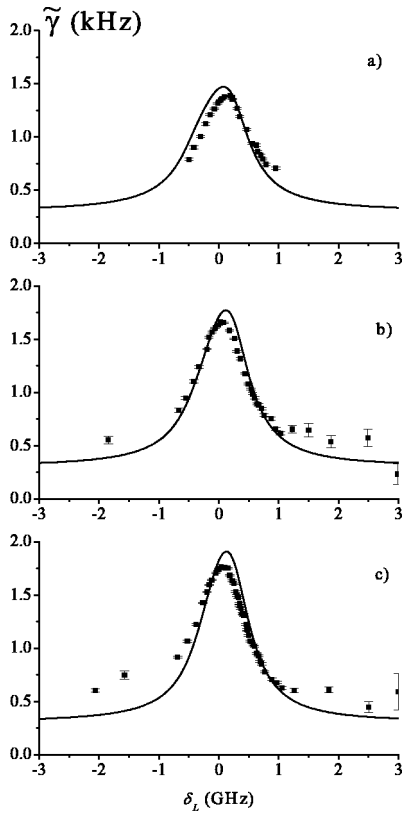

FIG. 6. Dark resonance width $\tilde{\gamma}$ versus optical detuning δ_L. Plots (a), (b), and (c) are for $\mathcal{R}=2.4$, 7.2, and 22, respectively. The solid lines indicate the theoretical predictions, while the points indicate the experimental data.

Thus, the results are qualitatively similar (the main differences are the overestimated amplitudes C_1 and C_2), but now all parameters are unambiguously defined for the actual atomic structure.

When $C_2=0$ the line shape is symmetrical, and occurs if $V=0$ or $\tilde{\Gamma}_1=\tilde{\Gamma}_2$. The first condition generalizes to $\delta_L=0$, and the second corresponds to the condition of equal Rabi frequencies in a simple Λ system.

When $V=0$, the amplitude of the symmetrical signal is proportional to the square of the two-photon coupling:

$$C_1 \approx \frac{2\,(\tilde{\Gamma}_1+\tilde{\Gamma}_2)^2}{\tilde{\Gamma}_{12}(\tilde{\Gamma}_1+\tilde{\Gamma}_2+Z\tilde{\Gamma}_1\tilde{\Gamma}_2)^2}U^2, \tag{29}$$

which is a key point of the perturbative studies [17] but now, in addition, all effects of the optical pumping are accounted for in the prefactor in Eq. (29).

VIII. DARK RESONANCE POSITION: THREE POSSIBLE DEFINITIONS

The center position of the dark resonance in essence determines the output frequency of the frequency reference or the magnetic field indicated by the magnetometer. Especially for asymmetrical resonances, it is somewhat unclear exactly how that center position is defined. The quantity δ_0 above is one possible definition of the resonance position, corresponding to the combined minimum of the absorptive part, and zero of the dispersive part, of the resonance described by Eq. (17).

Using Eqs. (18)–(22), one can easily find another possible definition of the resonance center: the Raman detuning corresponding to minimum absorption,

$$\delta_{\min}=S_1^{(0)}-S_2^{(0)}+\frac{\tilde{\Gamma}_{12}(\tilde{\Gamma}_2-\tilde{\Gamma}_1)}{\tilde{\Gamma}_1+\tilde{\Gamma}_2}\frac{V}{U}. \tag{30}$$

A third possible definition is the point y_0, where the dispersion n'_{DR} associated with the absorption (18) (by the Kramers-Kronig relations) is equal to zero. This is found to be

$$y_0=\delta_0-\frac{\tilde{\gamma}}{2}\frac{C_2}{C_1}. \tag{31}$$

Each of these three quantities, $\delta_{\min}$, y_0, and δ_0, could be considered the resonance center, depending on how the resonance is measured experimentally. In the general asymmetrical case, when $V\neq 0$ (nonzero effective one-photon detuning) and $\tilde{\Gamma}_1\neq\tilde{\Gamma}_2$ (unbalanced optical pumping rates), all

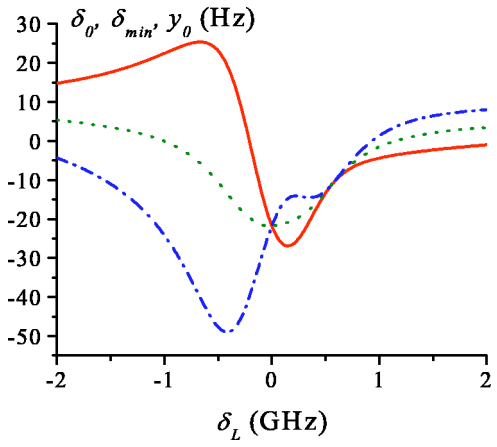

FIG. 7. Three possible definitions of the dark resonance position. The centroid δ_0 corresponds to the solid line, $\delta_{\min}$ corresponds to the dotted line, and y_0 corresponds to the dash-dotted line. All curves are calculated for the Cs D_2 line. The parameters are $\mathcal{I}=45\ \mu\mathrm{W/cm}^2$, $\mathcal{R}=0.5$, and $\gamma=2\pi 850$ MHz.

three values are different. Even their behavior versus δ_L is qualitatively different (Fig. 7), near the one-photon resonance ($V=0$) the centroid δ_0 of the Lorentzians has a dispersionlike shape, while $\delta_{\min}$ is rather of an absorptive nature, and y_0 has a more complicated shape of mixed type. In addition, δ_0 and $\delta_{\min}$ are always finite, whereas y_0 goes to infinity at the zeros of C_1. These different dependences on optical detuning could, for example, alter the sensitivity of the frequency reference or magnetometer to the optical lock point. As a result, careful consideration must be given to the resonance detection method while designing frequency references or magnetometers based on dark resonances.

IX. CONCLUSION

Using very simple assumptions about the relaxation processes, analytical results can be obtained for the nonlinear absorption of bichromatic radiation near a two-photon resonance. The theory fully takes into account both the HF and the Zeeman level structures of alkali-metal atoms, as well as all light-induced effects. Our results constitute a good basis for understanding experimental works, and further possible refinements of theory are possible. In particular, the case of large Doppler width $k\overline{v}>\gamma$ can be immediately studied by the substitution $\delta_L\rightarrow\delta_L-kv$ followed by averaging over the Maxwell distribution.

In addition, the theory allows for a simple parametrization of experimentally measured dark resonances in terms of absorptive and dispersive components. The theory can therefore predict, for example, the detuning for which the dispersive part of the resonance is minimized and, for a given detuning, the asymmetry in the resonance line shape that might be expected. The analysis of different definitions of the resonance center position is also of interest for practical applications based on dark resonances such as atomic frequency standards and magnetometers. It appears likely that the additional understanding gained by the thorough theoretical analysis presented here will lead to further refinement and development of current and future applications based on dark resonances.

ACKNOWLEDGMENTS

We thank S. Knappe, C. Affolderbach, I. Novikova, A. Matsko, and H. Robinson for helpful discussions. A.V.T. and V.I.Yu. were financially supported by RFBR (Grant Nos. 01-02-17036 and 03-02-16513).

APPENDIX: DERIVATION OF EQ. (6)

In this appendix we consider in detail the derivation of the basic equation set (6). As is well known the atomic density matrix obeys the generalized optical Bloch equation. According to this equation, the evolution of the density matrix can be split into two parts. The reversible one ($d/dt\,\hat{\sigma}=-i/\hbar[\hat{H},\hat{\sigma}]$) is governed by the total Hamiltonian of an atom in a resonant external field $\hat{H}=\hat{H}_0+\hat{H}_{D-E}$. The irreversible part originated from the interaction with environments (e.g., buffer gas or vacuum modes of electromagnetic field) are modeled by relaxation (super)operators of various kinds. The concrete form of the relaxation terms will be specified in the course of the derivation.

The first stage is the elimination of the optical coherences $\hat{\sigma}_{eg}=\hat{\Pi}_e\hat{\sigma}\hat{\Pi}_g$, where the operator $\hat{\Pi}_e=\Sigma_{m_e}|F_e,m_e\rangle\langle F_e,m_e|$ projects on the given HF component of the excited state. In the low-saturation limit, the optical coherence matrix obeys the following equation in the rotating frame:

$$\left[\frac{d}{dt}+\gamma/2-i(\delta_L-\omega_e)\right]\hat{\sigma}_{eg}$$

$$=\frac{i}{\hbar}\left\{\sum_{i=1,2}\hat{\Pi}_e(\hat{\mathbf{d}}\cdot\mathbf{E}_i)\hat{\Pi}_i\right.$$

$$\left.+\sum_{i\neq j}\hat{\Pi}_e(\hat{\mathbf{d}}\cdot\mathbf{E}_i)\hat{\Pi}_j e^{-i(\omega_i-\omega_j)t}\right\}\hat{\sigma}_{gg}. \quad \text{(A1)}$$

On the left-hand side, the Raman detuning δ_R is small compared to the homogeneous width γ ($|\delta_R|\ll\gamma$); $\hat{\Pi}_i=\Sigma_m|F_i,m\rangle\langle F_i,m|$, so that $\hat{\Pi}_g=\hat{\Pi}_1+\hat{\Pi}_2$. As is explained in the main text, the oscillations of the ground-state density submatrix $\hat{\sigma}_{gg}$ can also be safely neglected in the rotating frame. Then, in the stationary regime ($\gamma t\gg 1$) the solution of the equation (A1) is

$$\hat{\sigma}_{eg}=\frac{i}{\hbar}\left\{\sum_{i=1,2}\frac{\hat{\Pi}_e(\hat{\mathbf{d}}\cdot\mathbf{E}_i)\hat{\Pi}_i}{\gamma/2-i(\delta_L-\omega_e)}\right.$$

$$\left.+\sum_{i\neq j}\frac{\hat{\Pi}_e(\hat{\mathbf{d}}\cdot\mathbf{E}_i)\hat{\Pi}_j e^{-i(\omega_i-\omega_j)t}}{\gamma/2-i(\delta_L-\omega_e)-i(\omega_i-\omega_j)}\right\}\hat{\sigma}_{gg}. \quad \text{(A2)}$$

Under the conditions considered here, the equation for the ground-state density submatrix can be written as

$$\frac{d}{dt}\hat{\sigma}_{gg}=-\Gamma(\hat{\sigma}_{gg}-\hat{\sigma}_{gg}^{(0)})-\frac{i}{\hbar}[\hat{H}_0,\hat{\sigma}_{gg}]$$

$$-\frac{i}{\hbar}(\hat{\Pi}_g\overline{\hat{H}_{D-E}\,\hat{\sigma}}\hat{\Pi}_g-\text{H.c.})+\hat{\mathcal{A}}\{\hat{\sigma}_{ee}\},\quad \text{(A3)}$$

where the line over operators indicates time averaging, i.e., all the oscillating terms should be removed from the product $\hat{H}_{D-E}\,\hat{\sigma}$. Using Eq. (A2), one finds that

$$-\frac{i}{\hbar}\hat{\Pi}_g\overline{\hat{H}_{D-E}\,\hat{\sigma}}\hat{\Pi}_g=-i\,\hat{R}\,\hat{\sigma}_{gg},$$

where $\hat{R}$ is the excitation matrix given by Eq. (9). The first term on the right-hand side of Eq. (A3) describes the relaxation in the ground state (due to both diffusion and collisions) toward the equilibrium distribution outside the laser beam, $\hat{\sigma}_{gg}^{(0)}=\hat{\Pi}_g/n_g$. All the linear (with respect to $\hat{\sigma}_{gg}$) terms, containing Γ, $\hat{H}_0$, and $\hat{R}$, can be combined in the effective non-Hermitian Hamiltonian (8). The last term on the right-hand side of Eq. (A3) corresponds to the spontaneous radiative transfer of atoms from the excited states, given by the density submatrix $\hat{\sigma}_{ee}=\hat{\mathcal{P}}_e\,\hat{\sigma}\hat{\mathcal{P}}_e$ (where $\hat{\mathcal{P}}_e=\Sigma_{F_e}\hat{\Pi}_e$), to the ground-state levels. Its structure will be specified below.

In the low-saturation limit, the matrix $\hat{\sigma}_{ee}$ obeys the equation

$$\frac{d}{dt}\hat{\sigma}_{ee}=-\frac{1}{\tau_e}\hat{\sigma}_{ee}-\frac{i}{\hbar}[\hat{H}_e,\hat{\sigma}_{ee}]-\hat{\mathcal{G}}\{\hat{\sigma}_{ee}\}$$

$$-\frac{i}{\hbar}(\hat{\mathcal{P}}_e\overline{\hat{H}_{D-E}\,\hat{\sigma}}\hat{\mathcal{P}}_e-\text{H.c.}),\quad \text{(A4)}$$

where the first three terms on the right-hand side describe the radiative decay, the HF splitting ($\hat{H}_e=\hbar\Sigma_{F_e}\omega_e\Pi_e$), and the collisional depolarization of the excited state, respectively; the last term corresponds to the excitation due to light-induced transition from the ground-state levels. This last term can be considered as a source, because it is proportional to $\hat{\sigma}_{gg}$:

$$-\frac{i}{\hbar}\hat{\mathcal{P}}_e\overline{\hat{H}_{D-E}\hat{\sigma}}\hat{\mathcal{P}}_e$$

$$=\frac{1}{\hbar^2}\sum_{F_e,F_e'}\left(\sum_{i,j}\frac{\hat{\Pi}_{e'}(\hat{\mathbf{d}}\cdot\mathbf{E}_i)\hat{\Pi}_i\hat{\sigma}_{gg}\hat{\Pi}_j(\hat{\mathbf{d}}\cdot\mathbf{E}_j)^\dagger\hat{\Pi}_e}{\gamma/2+i(\delta_L-\omega_e)}\right.$$

$$\left.+\sum_{i\neq j}\frac{\hat{\Pi}_{e'}(\hat{\mathbf{d}}\cdot\mathbf{E}_i)\hat{\Pi}_j\hat{\sigma}_{gg}\hat{\Pi}_j(\hat{\mathbf{d}}\cdot\mathbf{E}_i)^\dagger\hat{\Pi}_e}{\gamma/2+i(\delta_L-\omega_e+\omega_i-\omega_j)}\right).$$

The structure of the collisional term $\hat{\mathcal{G}}\{\hat{\sigma}_{ee}\}$ can be found in Ref. [20]. Here we simply recall that during the course of a collision only the electronic component of the atomic polarization is depolarized. The nuclear component is involved in the process of depolarization due to the HF coupling. For all alkali-metal atoms, the excited-state HF splitting Δ_e is much greater than radiative decay rate $1/\tau_e$. In addition, we assume that the collisional relaxation rates γ_κ for the excited-state electronic multipole moments of rank $\kappa=1,\ldots,2J_e+1$ also obey the conditions $\gamma_\kappa\tau_e\gg1$ (for $\kappa=0$, we assume $\gamma_0=0$, i.e., the collision-induced transitions between the fine-structure components are not considered here). In this limit, $\Delta_e\tau_e\gg1$ and $\gamma_\kappa\tau_e\gg1$, the steady-state solution of Eq. (A4) has particularly simple form

$$\hat{\sigma}_{ee}=\pi_e\frac{\hat{\mathcal{P}}_e}{n_e},\quad \pi_e=\tau_e(i\,\text{Tr}\{\hat{R}\,\hat{\sigma}_{gg}\}+\text{c.c.}),\quad \text{(A5)}$$

which corresponds to total collisional depolarization of the excited state.

Here we shall illustrate this fact in one specific case, when the excited-state HF splitting is much larger than the depolarization rates γ_κ and when all the depolarization rates (except for γ_0) are the same (so-called pure electronic randomization model [20]). If $\Delta_e\gg\gamma_\kappa,1/\tau_e$, one can neglect HF coherence in the excited state. For pure electronic randomization both eigenvalues and eigenvectors of the Liouvillian $\mathcal{G}$ are well known [20], which allows us to write the steady-state solution of Eq. (A4) for arbitrary $\gamma_\kappa\tau_e$:

$$\hat{\sigma}_{ee}=\frac{\tau_e}{1+\gamma_\kappa\tau_e}\hat{S}_e+\frac{\gamma_\kappa\tau_e}{1+\gamma_\kappa\tau_e}\sum_{L,M,F_e,F_e'}\frac{\tau_e}{1+\tilde{\gamma}_L\tau_e}(-1)^{F_e-F_e'}\frac{(2F_e+1)(2F_e'+1)}{(2J_e+1)}\begin{Bmatrix}F_e & F_e & L\\ I & I & J_e\end{Bmatrix}$$

$$\times\begin{Bmatrix}F_e' & F_e' & L\\ I & I & J_e\end{Bmatrix}\hat{T}_{LM}(F_eF_e)\text{Tr}\{\hat{T}_{LM}^\dagger(F_e'F_e')\hat{S}_e\}.\quad \text{(A6)}$$

Here the source has the form

$$\hat{S}_e=\frac{\gamma}{\hbar^2}\sum_{F_e}\left(\sum_{i,j}\frac{\hat{\Pi}_e(\hat{\mathbf{d}}\cdot\mathbf{E}_i)\hat{\Pi}_i\hat{\sigma}_{gg}\hat{\Pi}_j(\hat{\mathbf{d}}\cdot\mathbf{E}_j)^\dagger\hat{\Pi}_e}{(\gamma/2)^2+(\delta_L-\omega_e)^2}+\sum_{i\neq j}\frac{\hat{\Pi}_e(\hat{\mathbf{d}}\cdot\mathbf{E}_i)\hat{\Pi}_j\hat{\sigma}_{gg}\hat{\Pi}_j(\hat{\mathbf{d}}\cdot\mathbf{E}_i)^\dagger\hat{\Pi}_e}{(\gamma/2)^2+(\delta_L-\omega_e+\omega_i-\omega_j)^2}\right),$$

the relaxation rates

$$\tilde{\gamma}_L=\gamma_\kappa\left[1-\sum_{F_e}\frac{(2F_e+1)^2}{(2J_e+1)}\begin{Bmatrix}F_e & F_e & L\\ I & I & J_e\end{Bmatrix}^2\right],$$

$$L=0,\ldots,2I+1 \tag{A7}$$

correspond to the Zeeman projections of the nuclear multipole moments of rank L [20], and the Wigner tensorial operators are defined as

$$\hat{T}_{LM}(F_a F_b)=\sum_{m_a,m_b}|F_a,m_a\rangle\sqrt{2L+1}\,(-1)^{F_a-m_a}\times\begin{pmatrix}F_a & L & F_b\\ -m_a & M & m_b\end{pmatrix}\langle F_b,m_b|.$$

As is seen from Eq. (A7), the rates $\tilde{\gamma}_L$ are of the order of γ_κ apart from $\tilde{\gamma}_0=0$. Then in the limit $\gamma_\kappa\tau_e\gg1$, the leading term of Eq. (A6) corresponds to the summand with $L=0$, which leads directly to the solution (A5).

When the excited-state HF coherence is negligible, the radiative repopulation term in Eq. (A3) can be written as

$$\hat{\mathcal{A}}\{\hat{\sigma}_{ee}\}=\frac{1}{\tau_e}\sum_{F_e,i,q}\frac{r(F_e,F_i)^2}{3}\hat{T}^\dagger_{1q}(F_e F_i)\,\hat{\sigma}_{ee}\hat{T}_{1q}(F_e F_i). \tag{A8}$$

One can easily prove the fundamental property

$$\hat{\mathcal{A}}\{\hat{\mathcal{P}}_e\}=\frac{1}{\tau_e}\frac{n_e}{n_g}\hat{\Pi}_g, \tag{A9}$$

which expresses the isotropy of the radiative relaxation.

Thus, we see that in the case of total collisional depolarization of the excited state, when the excited-state density matrix is proportional to $\hat{\mathcal{P}}_e$ [as shown in Eq. (A5)], Eq. (A3) is reduced to Eq. (6). In addition, the expression for the optical coherence matrix (A2) allows one to calculate various spectroscopic signals (as well as the total absorption), for example, the total dispersion.

[1] E. Arimondo, Prog. Opt. **35**, 257 (1996).
[2] R. Wynands and A. Nagel, Appl. Phys. B: Lasers Opt. **68**, 1 (1999).
[3] J. Kitching, S. Knappe, N. Vukićević, L. Hollberg, R. Wynands, and W. Weidemann, IEEE Trans. Instrum. Meas. **49**, 1313 (2000).
[4] M. Stähler, S. Knappe, C. Affolderbach, W. Kemp, and R. Wynands, Europhys. Lett. **54**, 323 (2001).
[5] S. Brandt, A. Nagel, R. Wynands, and D. Meschede, Phys. Rev. A **56**, R1063 (1997).
[6] M. Erhard and H. Helm, Phys. Rev. A **63**, 043813 (2001).
[7] S. Knappe, R. Wynands, J. Kitching, H.G. Robinson, and L. Hollberg, J. Opt. Soc. Am. B **18**, 1545 (2001).
[8] J. Kitching, L. Hollberg, S. Knappe, and R. Wynands, Electron. Lett. **37**, 1449 (2001).
[9] J. Kitching, S. Knappe, and L. Hollberg, Appl. Phys. Lett. **81**, 553 (2002).
[10] M. Stähler, R. Wynands, S. Knappe, J. Kitching, L. Hollberg, A. Taichenachev, and V. Yudin, Opt. Lett. **27**, 1472 (2002).
[11] E. Arimondo, Phys. Rev. A **54**, 2216 (1996).
[12] J. Vanier and C. Audoin, *The Quantum Physics of Atomic Frequency Standards* (Hilger, Bristol, 1989).
[13] A.S. Zibrov and A.B. Matsko, Phys. Rev. A **65**, 013814 (2001).
[14] M.D. Lukin, M. Fleischauer, A.S. Zibrov, H.G. Robinson, V.L. Velichansky, L. Hollberg, and M.O. Scully, Phys. Rev. Lett. **79**, 2959 (1997).
[15] H.Y. Ling, Y.-Q. Li, and M. Xiao, Phys. Rev. A **53**, 1014 (1996).
[16] B.A. Grishanin, V.N. Zadkov, and D. Meschede, Zh. Eksp. Teor. Fiz. **113**, 144 (1998) [JETP **86**, 79 (1998)].
[17] R. Wynands, A. Nagel, S. Brandt, D. Meschede, and A. Weis, Phys. Rev. A **58**, 196 (1998).
[18] S. Knappe, M. Stähler, C. Affolderbach, A. Taĭchenachev, V. Yudin, and R. Wynands, Appl. Phys. B: Lasers Opt. **76**, 57 (2003).
[19] N. Allard and J. Kielkopf, Rev. Mod. Phys. **54**, 1103 (1982).
[20] W. Happer, Rev. Mod. Phys. **44**, 169 (1972).
[21] N. Beverini, P. Minguzzi, and F. Strumia, Phys. Rev. A **4**, 550 (1971).
[22] R.H. Dicke, Phys. Rev. **89**, 472 (1953).
[23] S. Knappe, W. Kemp, C. Affolderbach, A. Nagel, and R. Wynands, Phys. Rev. A **61**, 012508 (2000).
[24] R. Wynands and A. Nagel, J. Opt. Soc. Am. B **16**, 1617 (1999).